Proc. Natl. Acad. Sci. USA
Vol. 83, pp. 6863–6867, September 1986
Cell Biology

Asymmetric lateral mobility of phospholipids in the human erythrocyte membrane

(phospholipid asymmetry/photobleaching/fluorescent phospholipids)

G. MORROT, S. CRIBIER, P. F. DEVAUX*, D. GELDWERTH, J. DAVOUST†, J. F. BUREAU, P. FELLMANN, P. HERVE, AND B. FRILLEY

Institut de Biologie Physico-Chimique, 13, rue Pierre et Marie Curie, 75005 Paris, France

Communicated by Pierre Joliot, June 2, 1986

ABSTRACT **The fluorescent phospholipid 1-acyl-2-[12-(7-nitrobenz-2-oxa-1,3-diazol-4-yl)aminododecanoyl]phosphatidylcholine (NBD-phosphatidylcholine) and the corresponding aminophospholipid derivatives (NBD-phosphatidylethanolamine and NBD-phosphatidylserine) were introduced in the human erythrocyte membrane by a nonspecific phospholipid exchange protein purified from corn. The lateral mobility of the fluorescent phospholipids was measured by using an extension of the classical photobleaching recovery technique that takes advantage of a modulated fringe pattern and provides a high sensitivity. In intact erythrocytes and in ghosts resealed in the presence of ATP, the fluorescence-contrast curves after photobleaching decayed biexponentially corresponding to two lateral diffusion constants. With NBD-phosphatidylcholine, the majority of the signal corresponded to a "slow" component (1.08×10^{-9} cm^2/sec at 20°C), whereas with the amino derivatives the majority of the signal corresponded to a "fast" component (5.14×10^{-9} cm^2/sec at 20°C). If the ghosts were resealed without ATP, the fast component of the aminophospholipids disappeared. We interpret these results as follows: (*i*) Provided the cells or the ghosts contain ATP, the three fluorescent phospholipids distribute spontaneously between inner and outer leaflets as endogenous phospholipids, namely NBD-phosphatidylcholine is located in the outer leaflet, while both aminophospholipids are preferentially located in the inner leaflet. (*ii*) The viscosity of the inner leaflet of human erythrocyte membranes is lower than that of the outer leaflet.**

ESR as well as fluorescence techniques have been used to assess the physical properties of the erythrocyte membrane. Several independent workers have suggested that the outer monolayer has a higher viscosity (1–3). However, the fluorescence polarization experiments by Schachter *et al.* (4) suggested a lower viscosity of the outer monolayer. Photobleaching experiments in turkey erythrocytes by Henis *et al.* (5) indicated identical lipid diffusibility in both layers below 24°C and higher lipid diffusibility in the external layer above 30°C. However, the same group reported a higher lipid diffusibility in the internal monolayer of human erythrocytes at 20°C and a higher lipid diffusibility in the external monolayer at 6°C (6). Thus the difference in lipid "mobility" or "fluidity" between inner and outer leaflets is still controversial.

There are several difficulties with these experiments. First, the selective probing of the inner and outer monolayer could introduce spurious effects. Henis and collaborators (5, 6) attempted to compare nonpermeant probes in intact cells and in leaky ghosts. The drawback of their method was to compare an intact cell with a modified system and assume arbitrarily that the membrane fluidity was not affected. An alternative approach is to compare the results obtained with selective probes of the inner or outer monolayer. In the native erythrocyte membrane, phosphatidylcholine (PtdCho) is located in the outer monolayer while phosphatidylethanolamine (PtdEtn) and phosphatidylserine (PtdSer) are located mainly in the inner monolayer (7). It was shown by several groups that exogenous phospholipids, when introduced in the erythrocytes, orient themselves as do endogenous phospholipids, providing the cells contain ATP (8–10). Therefore, in the present study we have employed fluorescent analogs of several naturally occurring phospholipids to probe separately the fluidity of the inner and the outer monolayers.

Another difficulty encountered, particularly when comparing different types of experiments, is a lack of rigor in the definition of the membrane fluidity. The mobility of a localized probe (either a spin labeled or a fluorescent lipid) may not reflect a macroscopic property of either membrane half. For example the environment of a probe attached to the head group of a phospholipid or near the methyl terminal of an alkyl chain can be very different and yet belong to the same monolayer. Besides, both paramagnetic and fluorescent probes reflect simultaneously local motions and order parameters (11, 12), and it is usually rather difficult to separate the contribution of each parameter. These restrictions do not apply to the measurements of long range lateral diffusion as determined by using photobleaching techniques. Indeed the rate of diffusion of a whole molecule is determined independently of the local wobbling of a residue.

The present article reports lateral diffusion measurements performed with phospholipids in ghosts and in intact erythrocytes. These fluorescent phospholipids have a 7-nitrobenz-2-oxa-1,3-diazol-4-yl (NBD) group at the C_{12} position of the β chain. They were incorporated into erythrocyte membranes via a nonspecific phospholipid exchange protein (13). The photobleaching apparatus used for this investigation is the modulated fringe pattern photobleaching setup described by Davoust *et al.* (14) and adapted to the observation of samples under a light microscope. The high sensitivity of this apparatus has allowed us to detect unambiguously two components of the diffusion with aminophospholipids incorporated in erythrocytes or in ghosts resealed in the presence of ATP.

MATERIALS AND METHODS

Fluorescent Phospholipids. 1-acyl-2-[12-(7-nitrobenz-2-oxa-1,3-diazol-4-yl)aminododecanoyl]phosphatidylcholine (NBD-PtdCho) and 1-acyl-2-[12-(7-nitrobenz-2-oxa-1,3-diazol-

The publication costs of this article were defrayed in part by page charge payment. This article must therefore be hereby marked "*advertisement*" in accordance with 18 U.S.C. §1734 solely to indicate this fact.

Abbreviations: NBD, 7-nitrobenz-2-oxa-1,3-diazol-4-yl; PtdCho, phosphatidylcholine; PtdEtn, phosphatidylethanolamine; PtdSer, phosphatidylserine; NBD-PtdCho, 1-acyl-2-[12-(NBD)aminododecanoyl]PtdCho; NBD-PtdEtn, 1-acyl-2-[12-(NBD)aminododecanoyl]-PtdEtn; NBD-PtdSer, 1-acyl-2-[12-(NBD)aminododecanoyl]PtdSer.

*To whom reprint requests should be addressed.
†Present address: European Molecular Biology Laboratory, Post fach 102209, D-6900 Heidelberg, Federal Republic of Germany.

4-yl)aminododecanoyl]phosphatidylethanolamine (NBD-PtdEtn) were purchased from Avanti Polar (Birmingham, AL). 1-acyl-2-[12-(7-nitrobenz-2-oxa-1,3-diazol-4-yl)aminododecanoyl]phosphatidylserine (NBD-PtdSer) was synthetized enzymatically from NBD-PtdCho by the method of Comfurius and Zwaal (15).

Preparation of Erythrocytes and Ghosts. Human blood was drawn from healthy donors into citrate/phosphate/dextrose buffer, stored at 5°C, and used within 5 days. Erythrocytes were washed five times with 145 mM NaCl/5 mM KCl/20 mM Hepes, pH 7.4 (buffer A). Pink, resealed ghosts were prepared by the method of Schwoch and Passow (16). Pink, resealed ghosts containing 3 mM ATP and a regenerating system (creatine phosphate and creatine kinase) were prepared as described in Seigneuret and Devaux (8). In several experiments the final washing of ghosts and erythrocytes was accomplished in 150 mM NaCl. In all instances, in the final buffer, $MgSO_4$ was avoided since Mg^{2+} inhibited the phospholipid exchange protein. Two types of leaky ghosts were prepared: white ghosts were obtained by using the method of Fairbanks *et al.* (17) that involves four extensive washings at low ionic strength before resuspending the membranes in isotonic buffer; pink, leaky ghosts were obtained as white ghosts except that the four extensive washings at low ionic strength were not included.

Membrane Labeling. Fluorescent phospholipid (5 μg), egg lecithin (5 μg), and cholesterol (5 μg) were dried in a glass tube. Then 500 μl of degassed buffer A was added to the dry lipids. The mixture was Vortex mixed and afterwards sonicated twice for 5 min with an Annemasse Sonifier, using a small titanium tip. The clear suspension was centrifuged at 40,000 × *g* for 30 min. Incubation was then as follows: 100 μl of the sonicated lipids were mixed with 25 or 50 μl of packed erythrocytes or ghosts, and 50 μl of buffer containing the exchange protein (1.9 mg/ml). The ratio of fluorescent lipids to endogenous lipids during incubation was thus around 1%. The incubation lasted 10–15 min at 30°C, then the membranes were washed with buffer A or 150 mM NaCl by three centrifugations at 20,000 × *g* in an Eppendorf centrifuge. Two microliters of the pellet was finally deposited on a glass plate and covered with a coverslip for light microscopic analysis. In some experiments the lipids were extracted after incubation and centrifugation, and the ratio of labeled lipids to endogenous lipids was determined.

Modulated Fringe Pattern Photobleaching. The principle of the modulated fringe pattern photobleaching has been described by Davoust *et al.* (14). The present apparatus is adapted to samples observed under a light microscope. A detailed description can be found in Davoust (18).

Briefly, an argon laser (Spectra Physics model 164-08), tuned to 488 nm was used as the excitation source for a fluorescence inverted microscope (Zeiss IM 35), provided with a home-built temperature control system based on a nitrogen gas flow regulating the temperature of the objective lens. A Mach–Zehnder interferometer served to split the excitation beam into two parts: the observation beam and the bleaching beam. The observation beam was attenuated by a factor of approximately 10^3 by successive reflection and passage through a dark filter. The bleaching beam was normally stopped by a microprocessor-controlled electromechanical shutter, which could be operated on command to deliver a brief (25–100 msec) unattenuated bleaching pulse. The two laser beams of unequal intensity were recombined into a single beam. Then, they were passed through a second interferometer constructed from a 50% beam splitter and two mobile mirrors mounted on piezoelectric ceramic (2 kHz modulation). The outcoming beams from the second interferometer were recombined so as to form interference fringes in the intermediate image plane of the microscope. Fringes were then produced through the objective lens on the sample. An oil-immersion objective lens with a magnification of ×63 was employed, allowing an interfringe spacing of 1 μm or less. The power on the sample during the bleaching pulse was ≈10 mW distributed over a total area of ≈0.038 mm^2. Thus the total dose for a 50-msec pulse was ≈1.1×10^{-3} $\mu J/\mu m^2$. Fluorescence emission light was collected again through the objective lens and sent through a dichroic mirror to the photomultiplier (Hamamatsu R1463-01). The signal from the photomultiplier was fed to a programmable double phase lock-in amplifer (Applications des Techniques Nouvelles en Electronique RDS II, Orsay, France) connected to a microcomputer (Victor S1).

This set-up enabled us to record the decay of the fluorescence contrast between bleached and nonbleached regions of the sample. Data were plotted either directly or after semilogarithmic transformation.

Simulation of the decay curves by one or two exponentials was performed systematically. A more elaborate analysis based on the exponential decomposition of the decay curves without any *a priori* assumption was also carried out. This latter method will be explained in a separate paper. The final determination of the ratio of the two components included a correction factor that took into account the finite bleaching time.

RESULTS

Sonicated vesicles containing a high ratio of fluorescent phospholipids were incubated with erythrocytes or with ghosts in the presence of the phospholipid exchange protein. The amount of incorporation determined by lipid extraction after centrifugation of the membranes revealed that a maximum of 20% of the incubated fluorescent lipids were finally associated with the erythrocytes, under our conditions of incubation. Hence, the ratio of fluorescent lipids to endogeneous lipids was in all instances ≤0.2% (≈0.4% if one assumes a selective incorporation in the outer monolayer). More quantitative details on the incorporation of labeled lipids in erythrocytes via the exchange protein will be published elsewhere. In agreement with the relatively low level of exogenous lipid incorporation, the cell morphology did not appear to be affected by the labeling. Adhesion of the erythrocytes to the glass plate, which is suggested by the absence of flow, was not accompanied by a shape change, at least during the time course of these experiments. It is important to notice that, as a consequence, all photobleaching experiments described below were carried out with normal discocyte cells.

Fig. 1*A* shows a typical contrast curve obtained in a single scan at 20°C with NBD-PtdSer in ghosts resealed in the presence of ATP. Between 300 and 200 cells are illuminated in one experiment. The simulated curve superimposed corresponds to the addition of two exponentials (see below). If I_o is the level of the signal intensity before bleaching, I_{max} the maximum intensity after bleaching, and I_∞ the level of the plateau, then $(I_\infty - I_o)/(I_{max} - I_o)$ gives an indication of the fraction of immobilized component. This fraction varied somewhat with the sample and with the area explored on the same microscope slide and depended upon the number of centrifugations carried out after membrane labeling. It does not seem to be representative of the nature of the labeled phospholipid. Typical values were between 5 and 25%.

Curves similar to those in Fig. 1*A* have been obtained with NBD-PtdEtn and NBD-PtdCho. Although similar, the curves are not identical. They are characterized by slightly different "apparent relaxation times." The curves displayed in Fig. 1 *B* and *C* have been obtained by the computer accumulation of several recordings performed on the same plate or on equivalent plates, maintained at 20°C. Fig. 1*B* corresponds to ghosts resealed in the presence of ATP while Fig. 1*C* corresponds to intact erythrocytes. Apart from an increase in noise in the latter experiments, results can be considered as

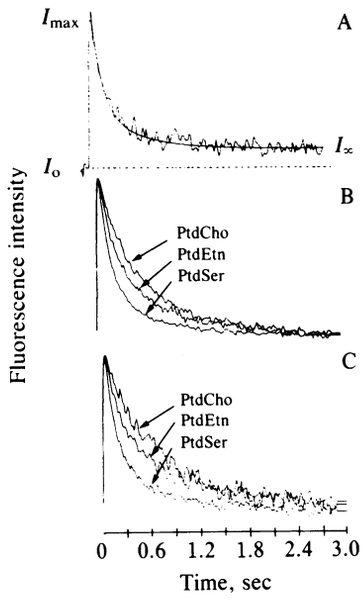

FIG. 1. Intensities of the modulated fluorescence, recorded after photobleaching (second harmonic) with various NBD-phospholipid derivatives in erythrocyte ghosts (*A* and *B*) and in erythrocytes (*C*). (*A*) A single recording obtained with NBD-PtdSer in ghosts resealed in the presence of 3 mM ATP (bleaching time, 25 msec; electronic time constant, 10 msec; interfringe spacing, 1.67 μm; the fraction of immobilized component, 15%). The full-line curve is a simulation obtained with two exponentials corresponding respectively to τ_1 = 110 msec and τ_2 = 650 msec; the fast component represents 85% of the signal in this simulation. (*B*) Accumulated recordings of NBD-PtdSer, NBD-PtdEtn, and NBD-PtdCho in ghosts resealed in the presence of 3 mM ATP (bleaching time, 50 msec; time constant, 10 msec; interfringe, 1.67 μm; number of accumulations: NBD-PtdSer, 10; NBD-PtdEtn, 17; NBD-PtdCho, 16). (*C*) Accumulated recordings in erythrocytes (number of accumulations: NBD-PtdSer, 21; NBD-PtdEtn, 26; NBD-PtdCho, 12). The curves displayed in *B* and *C* are normalized in such a way that I_{max} and I_∞ coincide. I_o is not shown for these accumulated curves since they were obtained with samples having a variable ratio of immobilized component.

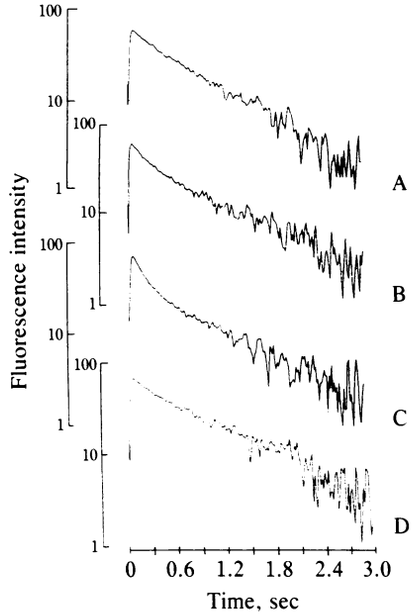

FIG. 2. Semi-logarithmic transformation of the fluorescence contrast curves after photobleaching obtained in ghosts. *A*, *B*, and *C* correspond to the transformation of the three accumulated curves displayed in Fig. 1*B* that were obtained with ghosts resealed in the presence of ATP. *A*, NBD-PtdCho; *B*, NBD-PtdEtn; *C*, NBD-PtdSer. *D*, NBD-PtdSer in ghosts resealed without ATP.

identical in ghosts and in erythrocytes. The important finding is that each phospholipid corresponds to a different relaxation time. The apparent time constant for the decrease in intensity varies in the following order: τ(NBD-PtdSer) < τ(NBD-PtdEtn) < τ(NBD-PtdCho).

However, as stated before, these curves, except perhaps for NBD-PtdCho, are not single exponentials. Fig. 2 *A–C* shows the semi-logarithmic transformation of the accumulated traces presented in Fig. 1*B*. If all curves could be fitted by an expression of the form:

$$I(t) - I_\infty = [I_{max} - I_\infty] \exp(-t/\tau), \quad [1]$$

a straight line would be obtained in the semi-logarithmic display. This is conceivable for NBD-PtdCho but certainly not for NBD-PtdEtn and NBD-PtdSer. Curve fittings as shown in Fig. 1*A* reveal that most decay curves can be fitted by two exponentials. The ratio of these two components depends upon the head group of the fluorescent phospholipid used. Both aminophospholipids (NBD-PtdEtn and NBD-PtdSer) give photobleaching contrast curves with a large contribution from a fast component. The results obtained at three different temperatures and the diffusion coefficient values are summarized in Table 1.

According to the theory developed by Davoust *et al.* (14), the diffusion coefficient D is related to the exponential decay time constant τ by the following formula:

$$D = i^2/(2\pi)^2\tau \quad [2]$$

where i is the interfringe spacing. The values of the diffusion coefficients shown in Table 1 correspond to the average of more than 10 measurements in each case. Data with ATP-containing ghosts and erythrocytes are compared. We found no significant differences between the ghosts and the intact cells. Note that the values appearing in Table 1 are unchanged if the photobleaching experiments are carried out immediately after the labeling step, which includes 15 min at 30°C, or if the labeling is followed by a several hour incubation at 4°C.

The same series of experiments were performed with ghosts resealed without ATP. This time the three fluorescent phospholipids gave, as a first approximation, one component, which corresponded to the slow component previously determined. In other words, the fast component disappears or is considerably reduced in the absence of ATP. This is illustrated in Fig. 2*D*. The same single exponential curve was obtained with NBD-PtdCho, NBD-PtdEtn, and NBD-PtdSer in ghosts resealed without ATP and in erythrocytes depleted of ATP by a several hour incubation at 37°C.

Fig. 3 shows a comparison of NBD-PtdCho incorporated in leaky ghosts obtained either after a mild treatment (*A*) or after extensive washing (*B*). In contrast to resealed ghosts, pink, leaky ghosts give rise to a two-component decay curve with NBD-PtdCho. However, with the white ghosts, i.e., with thoroughly washed cells, the two components are barely separable. Finally with all leaky ghosts, no difference could be detected between NBD-PtdCho, NBD-PtdEtn, and NBD-PtdSer (not shown).

DISCUSSION

The technique utilized in the present study was introduced by Davoust *et al.* (14), as an improvement of the classical fluorescence recovery after photobleaching (19, 20). A related static pattern photobleaching method has been introduced by Smith and McConnell (21) and used later by other investigators (22). It shows some of the advantages discussed here. The modulation existing in our system provides additional gain in sensitivity as well as very substantial improvement in data analysis.

Table 1. Lateral diffusion coefficients of fluorescent phospholipids in ghosts resealed with 3 mM ATP and in erythrocytes

Temp.	Fluorescent phospholipid	Membrane	Fast component, $(cm^2/sec) \times 10^9$	Slow component, $(cm^2/sec) \times 10^9$	% fast component
1°C	NBD-PtdCho	Ghosts	0.63 ± 0.07	0.14 ± 0.02	14 ± 8
		RBC	0.63 ± 0.14	0.11 ± 0.02	21 ± 8
	NBD-PtdSer	Ghosts	0.78 ± 0.06	0.11 ± 0.01	68 ± 8
		RBC	0.73 ± 0.11	0.09 ± 0.01	80 ± 8
	NBD-PtdEtn	Ghosts	0.53 ± 0.09	0.12 ± 0.02	60 ± 8
		RBC	0.45 ± 0.09	0.11 ± 0.03	44 ± 8
20°C	NBD-PtdCho	Ghosts	4.69 ± 0.79	1.17 ± 0.20	21 ± 10
		RBC	—	1.09 ± 0.37	≤10
	NBD-PtdSer	Ghosts	5.87 ± 0.58	1.07 ± 0.11	80 ± 10
		RBC	5.03 ± 0.84	0.91 ± 0.15	78 ± 10
	NBD-PtdEtn	Ghosts	4.69 ± 0.89	1.12 ± 0.21	57 ± 10
		RBC	5.41 ± 1.74	1.10 ± 0.35	50 ± 10
35°C	NBD-PtdCho	Ghosts	9.39 ± 1.64	1.90 ± 0.33	44 ± 15
		RBC	8.80 ± 1.48	1.41 ± 0.25	36 ± 15
	NBD-PtdSer	Ghosts	7.82 ± 1.18	1.76 ± 0.27	76 ± 15
		RBC	8.48 ± 1.97	1.35 ± 0.31	78 ± 15
	NBD-PtdEtn	Ghosts	8.80 ± 2.30	1.76 ± 0.46	60 ± 15
		RBC	7.82 ± 3.12	1.68 ± 0.67	56 ± 15

RBC, erythrocytes. The uncertainties of the diffusion coefficient include the mean deviations resulting from at least 10 decay curves plus an uncertainty related to the simulation of the curves by two exponentials. Finally the percentage of fast component includes an estimation of the uncertainty linked to the finite bleaching time. Note that the diffusion coefficients, at 1°C, corresponding to the "fast" component seem significantly different for PtdCho, PtdEtn, and PtdSer.

Pattern photobleaching is particularly adaptable to the study of erythrocytes, because erythrocytes have a relatively small size. With a spot photobleaching apparatus, only a very small area can be illuminated which, in turn, means collecting a low intensity of fluorescence. Averaging the noise by the repetition of many photobleaches on the same spot of an individual cell has been proposed as a means to improve the signal to noise ratio (23). However, by this procedure the same cell receives a high dose of damaging radiation. It is *a priori* more efficient to average the fluorescence of several hundred different cells, collected simultaneously by the pattern method. Not only does this technique increase the signal to noise ratio without increasing the time of measurement but also it permits one to average over many cells, thereby minimizing artifacts that may be due to a particular cell. In addition the light is distributed on a larger surface not only because many cells share the same laser beam but also because the fraction of the surface illuminated on each cell can be larger than with the spot technique. The total dose during bleaching ($\approx 1.1 \times 10^{-3}$ $\mu J/\mu m^2$) is approximately 20 times lower than values used in a classical photobleaching experiment (23).

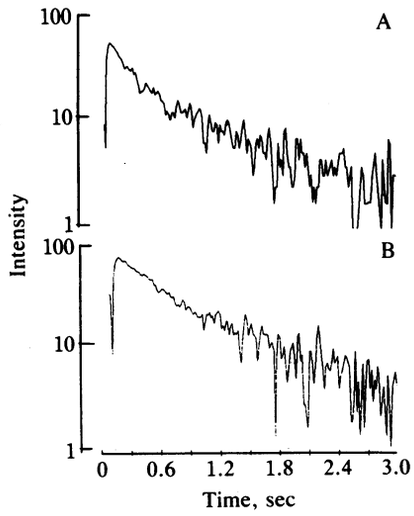

FIG. 3. Semi-logarithmic transformation of the fluorescence contrast curves after photobleaching obtained with NBD-PtdCho in leaky ghosts. Recording conditions as in Fig. 1. *A*, pink, leaky ghosts; *B*, white, leaky ghosts. The simulation of *A* indicates the presence of two exponentials ($\tau_1 \approx 164$ msec and $\tau_2 \approx 650$ msec; ratio of the two components, ≈50:50). *B* can be simulated as a single exponential decay with $\tau \approx 450$ msec.

An additional averaging can be obtained by collecting several recordings of the same type of experiment. In practice the accumulation of approximately 10 photobleaches on different areas of the same plate or of related plates means a total of approximately 2500 cells averaged within a few minutes, with a consecutive signal to noise ratio improvement of ≈50-fold over a classical photobleaching recovery experiment. That is without considering the benefit in signal to noise ratio due to the modulation and phase detection of the signal.

The present technique offers also significant advantages from the viewpoint of the data analysis. The time dependence of the intensity of the second harmonic, for a single diffusion process, follows a single exponential law rigorously. Thus a straightforward linearization is obtained by semi-logarithmic transformation of the signal.

In principle, Eq. 2 is only valid when an infinite number of fringes cover the same cell (14). Fortunately, Davoust has shown that five or six fringes are sufficient in practice (18). The interfringe spacings used in our experiments were between 1.5 and 1.9 μm, which gives, with erythrocytes, a sufficient number of fringes. Decreasing *i* further would imply having very short τ values and, therefore, would require extremely short bleaching times. In fact we could never work with a bleaching time negligible in comparison with τ because of sensitivity problems. This has a consequence in the determination of the fraction of the two components (but not in the determination of τ values). It explains the relatively high uncertainty in the determination of the percentage of fast component (see Table 1).

The Immobilized Fraction. The "immobilized fraction" is often referred to as the lipids in strong interaction with membrane proteins forming long-lived complexes. However, we think that, at least in the experiments described in this article, a much simpler and more likely explanation is that the immobilized lipids are not incorporated in the erythrocyte membranes. The immobilized fraction would correspond to the fluorescence emitted by sonicated vesicles that adhere to the erythrocyte membranes without actually fusing. Since the diameter of these vesicles is much smaller than the interfringe spacing, they give rise to an apparent immobile fraction. One may ask why these vesicles still fluoresce in spite of the high concentration of fluorescent lipids, which would normally lead to fluorescence quenching. The following two explanations are proposed: (*i*) the samples have been exposed to an exchange protein that dilutes the labeled lipids, and (*ii*) the bleaching beam destroys a fraction of fluorescent lipids. Both effects should allow the sonicated vesicles to fluoresce. In conclusion we think that these "immobilized lipids" are not representative in any way of the lipid mobility within erythrocyte membranes.

Interpretation of the Diffusion Results in Erythrocytes. Table 1 shows that in ghosts loaded with ATP and in the native erythrocytes, the fast diffusing component corresponds to the major fluorescent fraction when using aminophospholipids and to a minor fraction when using the phosphatidylcholine derivative. For each specific phospholipid, the percentage of fast diffusing component is similar to the percentage of the naturally occuring phospholipid in the inner monolayer (7). A reasonable conclusion is that the lipid diffusibility is high in the inner monolayer and low in the outer monolayer. It follows that the results can be explained within the framework of the model proposed previously by our group, on the basis of spin label data in erythrocytes (3, 8). The interpretation is as follows: (*i*) The lipids incorporated in the sealed erythrocyte membrane either by protein-stimulated exchange or spontaneous partition, are incorporated initially in the outer monolayer where they diffuse laterally with a diffusion coefficient equal to 1.08×10^{-9} cm^2/sec at 20°C. (*ii*) Provided the ghosts or the erythrocytes contain ATP, NBD-PtdSer and, to a lesser extent, NBD-PtdEtn are rapidly transported towards the inner layer where they diffuse laterally with a diffusion coefficient equal to $\approx 5.14 \times 10^{-9}$ cm^2/sec at 20°C. (*iii*) As opposed to the amino derivatives, NBD-PtdCho stays essentially in the outer monolayer. In the absence of ATP all the three exogenous phospholipids stay in the outer monolayer. (*iv*) With leaky ghosts, labeled lipids distribute between both layers regardless of the nature of the phospholipid head group and give rise to photobleaching decay curves with two components. However, very likely, extensive centrifugation and washing that are required for the preparation of "white ghosts" are accompanied by a redistribution of the endogenous lipids and, hence, the asymmetry of the viscosity is lost (24).

The present data confirm our findings with spin labeled lipids, (*i*) that the reorientation of the aminophospholipids in erythrocytes is an ATP-dependent phenomenon and (*ii*) that the viscosity of the inner monolayer is lower than that of the outer monolayer in the native erythrocyte membrane.

Comparison with Other Photobleaching Results in Erythrocytes. The lateral mobility of fluorescent lipids in human erythrocyte membranes has been investigated by several groups, by using the spot photobleaching technique (23, 25–27). Different groups have used different probes as well as different techniques of incorporation. The results range from 1.6×10^{-9} cm^2/sec to 8.2×10^{-9} cm^2/sec at ≈20°C. Bloom and Webb (23) have discussed several pitfalls of the technique that might explain the discrepancies. The same authors were able to compare the diffusion constants in resealed ghosts and in intact cells (23). For this purpose they used Di I(5) (3,3'-dioctadecyl indodicarbocyanine iodide), which is not a phospholipid. Optical absorption due to intracellular hemoglobin was avoided by using excitation of Di I(5) at 647 nm. The diffusion constants at 25°C were found to be very close: 8.2×10^{-9} cm^2/sec for intact cells and 7.8×10^{-9} cm^2/sec in resealed ghosts. Our results are in agreement, in the sense that we find no significant difference between resealed ghosts and intact cells.

All previous investigators have calculated a single diffusion coefficient associated with each fluorescence recovery curve. This is because the sensitivity and the theoretical analysis of a spot photobleaching recovery curve do not permit the separation of two close components. In fact the procedures employed for the incorporation as well as the nature of the labeled lipids suggest that in most earlier investigations, only the external monolayer had been probed. We have shown that only with very specific probes (such as the PtdSer analog and in this case only if ATP is contained in the cell) can one investigate the inner monolayer of erythrocytes. The present article at least qualitatively confirms the findings of Rimon *et al.* (6) concerning the asymmetry of lipid diffusibility in erythrocyte membranes at high temperature, but does not support their statement about the inversion of this asymmetry at low temperature. Possibly the difference is due to their using leaky ghosts.

The authors thank Dr. J. C. Kader for the gift of the phospholipid exchange protein and Drs. J. Aubard and P. Levoir for the analysis of the decay curves in several exponentials. This work was supported by grants from the Ministère de la Recherche et de la Technologie, the Centre National de la Recherche Scientifique (UA 526), the Institut National de la Santé et de la Recherche Médicale, the Université Paris VII, and the Fondation pour la Recherche Médicale.

1. Tanaka, K. I. & Ohnishi, S. I. (1976) *Biochim. Biophys. Acta* **426,** 218–231.
2. Williamson, P., Bateman, J., Kozarsky, K. & Mattocks, K. (1982) *Cell* **30,** 725–733.
3. Seigneuret, M., Zachowski, A., Hermann, A. & Devaux, P. F. (1984) *Biochemistry* **23,** 4271–4275.
4. Schachter, D., Cogan, U. & Abbot, R. E. (1982) *Biochemistry* **21,** 2146–2150.
5. Henis, Y. I., Rimon, G. & Felder, S. (1982) *J. Biol. Chem.* **257,** 1407–1411.
6. Rimon, G., Meyerstein, N. & Henis, Y. I. (1984) *Biochim. Biophys. Acta* **775,** 283–290.
7. Van Deenen, L. L. M. (1981) *FEBS Lett.* **123,** 3–15.
8. Seigneuret, M. & Devaux, P. F. (1984) *Proc. Natl. Acad. Sci. USA* **81,** 3751–3755.
9. Daleke, D. L. & Huestis, W. H. (1985) *Biochemistry* **24,** 5406–5416.
10. Tilley, L., Cribier, S., Roelofsen, B., Op den Kamp, J. A. F. & Van Deenen, L. L. M. (1986) *FEBS Lett.* **194,** 21–27.
11. Schreier, S., Polnaszek, C. F. & Smith, I. C. P. (1978) *Biochim. Biophys. Acta* **515,** 375–436.
12. Heyn, M. D. (1979) *FEBS Lett.* **108,** 359–364.
13. Kader, J. C., Julienne, M. & Vergnolle, C. (1984) *Eur. J. Biochem.* **139,** 411–416.
14. Davoust, J., Devaux, P. F. & Léger, L. (1982) *EMBO J.* **1,** 1233–1238.
15. Comfurius, P. & Zwaal, R. F. A. (1977) *Biochim. Biophys. Acta* **488,** 36–42.
16. Schwoch, G. & Passow, H. (1973) *Mol. Cell. Biochem.* **2,** 197–218.
17. Fairbanks, G., Steck, T. L. & Wallach, D. F. H. (1971) *Biochemistry* **10,** 2606–2617.
18. Davoust, J (1983) Thèse de Doctorat d'Etat (Université Paris VI, Paris, France).
19. Peter, R. (1981) *Cell Biol. Int. Rep.* **5,** 733–760.
20. Vaz, W. L. C., Derzko, Z. I. & Jacobson, K. A. (1982) in *Membrane Reconstitution*, eds. Poste, G. & Nicolson, G. L. (Elsevier, Amsterdam), pp. 83–136.
21. Smith, B. A. & McConnell, H. M. (1978) *Proc. Natl. Acad. Sci. USA* **75,** 2759–2763.
22. Koppel, D. E. & Sheetz, M. P. (1983) *Biophys. J.* **43,** 175–181.
23. Bloom, J. A. & Webb, W. W. (1983) *Biophys. J.* **42,** 295–305.
24. Dressler, V., Haest, C. W. M., Plasa, G., Deuticke, B. & Erusalimsky, J. D. (1984) *Biochim. Biophys. Acta* **775,** 189–196.
25. Kapitza, H. G. & Sackmann, E. (1980) *Biochim. Biophys. Acta* **595,** 56–64.
26. Thompson, N. L. & Axelrod, D. (1980) *Biochim. Biophys. Acta* **597,** 155–165.
27. Golan, D. E., Alecio, R. M., Weatch, W. R. & Rando, R. R. (1984) *Biochemistry* **23,** 332–339.